Influence of Localized Rainfall Patterns on Landslide Occurrence: A Case Study of Southern Hiroshima with XRAIN Data During the July 2018 Heavy Rain Disasters

Dos Santos Rodrigues Neto José Maria
Ehime University
Netra Prakash Bhandary (netra@ehime-u.ac.jp)
Ehime University

Research Article

Keywords: Localized rainfall, landslides, XRAIN data, July 2018 heavy rain disasters

Posted Date: March 16th, 2022

DOI: https://doi.org/10.21203/rs.3.rs-1446935/v1

Abstract

The landslide problem in Japan was exemplified by the July 2018 landslides and flood disasters in Southwestern Japan induced by extremely heavy rainfall. In this study, GIS and other analytical platforms were utilized to analyze landslide distribution patterns in the July 2018 heavy rain disasters around the city of Kure (Southern Hiroshima) in conjunction with chronological XRAIN (eXtended Radar Information Network) radar-acquired localized rainfall data in order to achieve a better understanding of the relationships between rainfall characteristics and landslide probability and to investigate the potentials of radar-acquired rainfall data in landslide susceptibility study approaches. Analysis of the rainfall data demonstrates that mean annual precipitation in the whole study area ranges between 2,004 mm and 2,961 mm, with an average of about 2,152 mm for the whole extension of the area. Observation of the spatial distribution of rainfall volumes throughout the sampled years shows that rainfall is remarkably localized, with higher values concentrated on elevated areas. It is observed, however, that the peak rainfall volumes are not so closely related to landslide occurrence. Analysis of event rainfall from the July 2018 disasters determines that landslide-inducing rainfall started from 8:30 AM on July 5th and continued with a mean intensity of 7.8 mm/h for about 47 hours until 7:30 AM of July 7th, accumulating to up to 368 mm in total and that there were two intensity peaks, one around 7:30 PM on the night of July 6th, and another one around 4:30 AM on July 7th. These two events are associated with particularly high landslide activity, which indicates that landslide activation is related to peak intensity rainfall combined with accumulated continuous precipitation. This study demonstrates a clear association of landslide activity with heavy rainfall both in spatial and chronological aspects, weighing into the evidence that rainfall intensity, timing, and spatial distribution are true of vital relevance for landslide occurrence.

1. Introduction

Landslide disasters occur very frequently worldwide causing substantial human loss and property damage (Geertsema et al., 2009, Yilmaz, 2009, Petley, 2012; Centre for Research on the Epidemiology of Disasters, 2017). Such events are predisposed by various physical factors inherent to the slope in question, such as geology, geomorphology, steepness, drainage system and others (Guzzetti et al., 1996; Dai et al., 2002), but the major triggering factor in most of the cases is rainwater infiltration (Osanai et al, 2009). Most of the landslide disasters around the world happen during the rainy seasons of the respective region, such as January in South America (Canavesi et al., 2013) or July in Japan (Matsushi et al., 2014). The problem of rain-induced landslides in Japan was exemplified during the July 2018 heavy rain-induced disasters in west Japan including in the city of Kure, in Hiroshima Prefecture (Fig. 1).

Landslides and floods triggered by the heavy rains, officially referred to as "Heavy Rains of July 2018" were the main causes of the disasters. In the course of about 10 days from 28 June until 8 July, the rainfall records reached as much as 1800 mm on the island of Shikoku and 1200 mm in Tokai region. Many cities recorded more than 400 mm of rainfall in the course of 72 hours (Japan Meteorological Agency, 2018).

In Hiroshima Prefecture, one of the most affected areas was Kure, with 10 people deceased due to landslides. Additionally, most transportation lines into the city (except maritime ways) were cut off and 760 houses were damaged (Fig. 2).

Southern Hiroshima Prefecture is occasionally affected by heavy rain-induced landslide and flooding disasters, such as in 1999 (Chigira, 2001; Ushiyama et al., 2001), 2014 (Matsushi et al., 2014) and 2018. A common factor for all of the mentioned landslide disasters in the city is that these occurred during periods of continuous heavy rain between June and July, a fact that points out the substantial role of rainfall in landslide occurrence. Although necessary for the predisposition of a slope to lose its stability and fail, landslides rarely occur only with predisposed factors such as geology, soil condition, slope geometry, etc. A triggering mechanism is considered necessary to spark the final break of stability and consequently, mass movement (Highland & Bobrowsky, 2008). The most common trigger in the majority of landslide-affected areas all around the world is break of slope stability caused by pore water density and saturation increase led by unusually heavy rainfall (Guidicini & Isawa, 1977; Caine, 1980; Chigira, 2001; Guzzetti et al., 2007; Dahal & Hasegawa, 2008; Highland & Bobrowsky, 2008; Dahal, 2012; Wang et al., 2015; and others).

In landslide hazard assessment studies, rainfall data usually comprise of mean annual precipitation data collected via rain gauge stations. Typically, each station is referent to a whole municipality, and is located near city centers. In the case of the study area, Japan Meteorological Agency (JMA) has a measurement station in downtown Kure, with the other nearest stations being at Kurahashi, 16 km southwards, and Hiroshima, 18 km northwest. Slope failure assessment analysis using rainfall data have been widely investigated in the literature, including for the present study area (Ushiyama et al., 2001; Matsushi et al., 2014). However, rain gauge stations gather information in the scale of whole municipalities may not be representative of the actual spatial distribution of precipitation in a degree of detail considered ideal for various methods of slope failure assessment. In reality, rainfall intensity values may vary in the order of less than hundreds of meters, especially in areas with rugged mountainous terrain or coastal regions. However, recent advancements in radar technology such as XRAIN (eXtended RAdar Information Network) data have allowed for instant measurement of rain intensity in much more detailed scales of spatial distribution.

In view of the need of more thorough analysis of rainfall patterns and their relationship and relevance with landslide disasters, this analytical work aims at investigating rainfall data in the study area of Kure City (Southern Hiroshima Prefecture, Southwestern Japan) in the context of the July 2018 landslide disasters, using innovative XRAIN radar-acquired rainfall data. The research plans to correlate landslide occurrence (during the July 2018 disasters) with rainfall volume distribution in varied time windows in search of localization patterns. The identification of such patterns may evidence effectiveness of XRAIN radar-acquired rainfall data in landslide hazard assessment, as well as lead to better understanding of the effects of rainfall in landslide activation and probability which may contribute to better strategies in landslide disaster prevention methods.

2. Material And Method

2.1. Study area

The area analyzed in this research comprises of a 390.5 km^2 rectangle around the municipality of Kure, in Southern Hiroshima (Fig. 1). Stranded between the Hiroshima Mountains at north and the Seto Inland Sea to the south, the city is a small shipbuilding town which experienced rapid growth in the first half of the 20th century, which forced urbanization in areas at or adjacent to the mountainous terrain.

The mountains are mostly composed by volcanic rocks, namely rhyolites and granites/granodiorites from the Hiroshima Group (Yamada et al., 1986). When weathered, these rocks change into a soil commonly referred to as Masado, which is known to be highly permeable and become very brittle when wet, configuring a material very prone to slope failure during rainfall events (Wang et al., 2015). This setting, fairly common around the country's coastline, makes the city a potential high-risk area for landslide disasters. A digital elevation model (DEM) along with landslide occurrence during the July 2018 event is exhibited in Fig. 3.

The Seto Inland Sea (which Kure is adjacent to) has little rainfall compared to the surrounding oceanic coastal areas in Japan, like the Sea of Japan and the Pacific Ocean. Although a fairly good part of the oceanic precipitation clouds is blocked either by the Chugoku mountains northward or the Shikoku mountains southward and the region relatively dry (Kamada & Nakagoshi, 1996), heavy rainfall is particularly concentrated in mountainous areas. In Kure, the average annual average precipitation ranges from 1,000 to 1,600 mm, characterizing a relatively mild rainy zone. Mountain areas around the Seto Inland Sea, however, reach annual average precipitation of 2000 mm to 3000 mm. The period of the year with the heaviest rainfall occurs between June and July every year, when the average precipitation reaches 227 mm (Japanese Meteorological Agency, 2020).

2.2. XRAIN radar-acquired rainfall data

XRAIN radar technology started to be utilized in Japan in the year of 2014, operated by the country's Ministry of Land, Infrastructure, Transport and Tourism. The technology used in the measurements differs from common radar rainfall data since it uses Multi-parameter (MP) radars, which allow for more accurate measurements of rainfall volume.

Although being arguably not as quantitatively accurate as regular rain gauge measurements, radar-based rainfall measurement methods have the advantage of being performed over a bi-dimensional "planar" area, where each pixel in the area's grid represents a specific value, whereas rain gauge methods extrapolate the value of a single measurement station over extensive regions. This means that radar-acquired data allows for rainfall distribution analysis in a larger scale.

XRAIN data are represented in 287x230 m pixel grids, where each pixel's value represents the rainfall intensity in mm/h for the referred location in the time of measurement, which happens every 1 minute. The data are obtainable from the Data Integration & Analysis System (DIAS) platform, which is operated

by the University of Tokyo and sponsored by the Ministry of Education, Culture, Sports, Science and Technology (MEXT). The measurement spacing can be set as 1, 5, 10, 15, 30 and 60 minutes.

Although XRAIN raw data expresses rainfall momentary intensity, precipitation volume can be estimated by the calculation of intensity during a specified period of time either by averaging the measurements over that period and multiplying it by the number of times that the measurement interval is repeated in it, or simply by summing the intensity values in the case of a 1-hour interval analysis with no missing measurements.

For this work, the XRAIN data were downloaded as *.zip packed *.csv files spaced in 5-minute, 30-minute or 1-hour intervals. The *.csv files comprise of tables with cells spatially organized so that each cell represents a 287 x 230 m pixel in a north-oriented grid representing the designated area, and each cell's value expresses the rainfall intensity in mm/h at the time of measurement. For the study area, each of the files comprised of a 97 x 67 grid with 4999 pixels. XRAIN data collection for the area of Chugoku (where Kure is located) started at 2016, so the range of collected data spans from 2016 to 2019, summing up to more than 40,000 .csv files. These files were combined in single worksheets in Microsoft Excel for calculations, analyses, and conversions into ArcGIS shapefiles.

2.3. Data analysis

After proper conversions, the data were jointly analyzed with the use of ArcGIS Pro software for localization and spatial distribution inspections and Microsoft Excel for other statistical analysis and graph visualization of data. The investigation methods include determining average accumulation throughout the analyzed time windows (from 2016 to 2019) for the whole study area as well as its spatial distribution; calculating landslide density based on precipitation classes; constructing a timeline of rainfall intensity in the study area (and its spatial distribution) during the period of rainfall pertaining to the July 2018 disasters; assessing a spatial relationship between landslide occurrence and rainfall.

3. Results And Discussion

3.1. Mean annual rainfall accumulation

Upon inspecting the annual rainfall accumulation numbers in the study area throughout the years of 2016 to 2019, it was noted that mean rainfall accumulation amounts to an average of 2151.9 mm per year, with maximum value in the area of 2961.1 mm and a minimum value of 2004.1 mm. The accumulation values for each of the years are 2954.8 mm for 2016, 2108.7 mm for 2017, 2456.3 mm for 2018, and 1847.9 mm for 2019. Although these values greatly differ from Japan Meteorological Agency (2020) mean annual rainfall results of only 1381 mm per year for Kure's rain gauge station, it is noticeable that the rainfall history from 2016 to 2019 follows the exact same patterns as the JMA values for these years: 1925 mm for 2016, 1359.5 mm for 2017, 1757 mm for 2018, and 1215 mm for 2019. The JMA rain gauge values for Kure city every year are lower than XRAIN radar values in the order of about 0.7.

This may be explained either by differences in the rainfall measurement sampling area, since JMA's measurement station for Kure City is located in downtown Kure near the port, a low topographical area with relatively low rainfall volumes throughout the year when compared to the rest of the study area. However, when checking the localized rainfall values for the location of the JMA measurement station, although the precipitation value is relatively lower than the XRAIN mean data, it still exceeds the rain gauge measurements in about 500 mm. Or yet, it is also possible that the nature of radar-acquired rainfall measurements such as XRAIN actually exaggerates rainfall measurements, returning values co-relatable however disparate of rain gauge station measurements.

Concerning localization aspects of the annual rainfall accumulation, all year data present similar spatial patterns (Figs. 4 and 5), where peak values are concentrated around Mt. Noro, at the central east part of the area, and subordinately Mt. Enofuji, at the central west part of the area. Minimum values, on the other hand, are concentrated in the topographically low valleys where central Kure and Yakeyamachuo area is located. The aspect that heavier rainfall volumes are concentrated in topographically elevated areas is fairly noticeable when comparing localization patterns with topographical values. This relationship is further illustrated in the graph and map of Fig. 6.

Comparing the localized rainfall aspects and the occurrence of landslides in the area during the 2018 disasters, a relationship between peak rainfall values and landslide activity is fairly noticeable, especially around the northern flank of Mt. Noro, and Mt. Enofuji, where landslide occurrence was particularly significant. The co-relation is not so fitting, however, in the extreme northwestern region of the area around Mt. Ege, where landslide occurrence was significant even though mean annual rainfall accumulation values are not so high in the area.

The relationship between rainfall accumulation values and landslide occurrence is illustrated in Table 1 as well as the graph of Fig. 7, where landslide density per rainfall class is compared to rainfall volumes (areas with slope degrees lower than 20 and higher than 50 were excluded from analysis for better landslide co-relation). It is noticeable that, as expected, landslide occurrence increases according to rainfall value. However, there is a sudden decrease of landslide density in classes of extremely high rainfall volumes. This may be explained simply by the fact that sampling area is very small for extreme rainfall values, causing statistical error. Moreover, these high rainfall volumes are typically concentrated in high topographical areas, which are not so prone to landslides since the slopes in these regions are usually composed of summits weathered down to bedrock. This demonstrates that localized rainfall volume, even when analyzed in long ranges such as yearly volumes instead of in single event ranges, is co-relatable with landslide occurrence.

Table 1
– Number of landslides per mean annual precipitation (MAP) ranges in intervals of 50 mm, along with the area for each respective MAP range in the study area, as well as its resultant landslide density.

MAP range (mm)	Class area (km^2)	Number of landslides	Landslide density (/km^2)
< 2100	6.87	14	2.03
2100–2150	23.31	67	2.87
2150–2200	34.75	79	2.27
2200–2250	39.44	178	4.51
2250–2300	34.43	246	7.14
2300–2350	13.39	117	8.73
2350–2400	9.31	130	13.96
2400–2450	6.29	64	10.17
2450–2500	5.63	54	9.58
2500–2550	4.39	67	15.24
2550–2600	3.36	37	10.99
2600–2650	4.04	40	9.89
2650–2700	2.49	14	5.6
> 2700	3.16	21	6.63

3.2. Rainfall on the July 2018 disaster event

Inspection of XRAIN chronological data of the time before and leading to the landslide disasters at Kure City shows that Kure was experiencing a rest of substantial rainfall since 7 AM of July 4th, when Category 1 Typhoon Prapiroon (TY 1807) was weakening into a low-pressure area as it advanced to northeastern Japan, leaving the city to a mildly good and sunny weather. The weather maintained for about 25 hours until 8:30 AM of July 5th, when heavy rainfall clouds approaching from southwest landed on Honshu, laying the city into a continuous heavy rainfall situation for about 2 days, a condition which would eventually lead to the landslides in the night of July 6th and early morning of July 7th, after which the heavy rainfall finally ceased, and the weather was relatively clear for the whole following day.

Analysis of rainfall data of the event for the study area shows that in the period of 47 hours between July 5th 8:30 AM (start of rainfall) until July 6th 7:30 AM (end of rainfall), the event rainfall followed the general MAP spatial distribution (Fig. 8).

Analysis of average rainfall values for the whole study area allows for chronological interpretations in the case of an isolated event. Taking this approach, it was noted that the average rainfall in the study area

was of 7.8 mm/h, and the total cumulative rainfall was of 368 mm. There were two particular peaks of rainfall intensity, one around 7:30 PM of July 6th (35 hours into the event) with an intensity of 47 mm/h, and another at 4:30 AM of July 7th (44 hours into the event) when rainfall intensity reached 40 mm/h (Fig. 9).

Checking news and records of landslides during the disasters, it is found that landslides were recorded around 19:40 PM of July 6th (Japan Meteorological Agency, 2018), and then again in greater numbers around 5 to 6 AM of July 7th (Ministry of Land, Infrastructure, Transport and Tourism, 2018). These two main landslide occurrence reports will hereinafter be called “subevent 1” and “subevent 2”, respectively. Checking the XRAIN rainfall intensity history in Fig. 9, it is noticeable that these two subevents coincide directly with the rainfall intensity peaks around 7:30 PM of July 6th and 4:30 AM of July 7th. This points out that, as expected, landslide triggering is probably related to peak intensity rainfall, and that – since the rainfall intensity in subevent 2 is lower than in subevent 1 – the intensity threshold for landslide activation is lower when there is longer duration cumulative rainfall.

When checking the rainfall history graph for each of the study area’s 67 longitudinal cells along a profile on the area’s latitudinal center line (Fig. 10), however, it is noticeable that the rainfall peak’s timing varies according to the measurement’s cell longitudinal position. At the farthest western measurement cell of the study area (blue tones in Fig. 10), the rainfall intensity peak happens about 1 hour before the same intensity peak at the farthest eastern measurement cell (white tones at Fig. 10). The same pattern is also noticed in subordinate intensity peaks during the rainfall history, mainly around 8 hours and 47 hours into the event. This demonstrates an eastward movement of the rainfall front and intensities in this particular event dislocating about 28 km (the study area’s longitudinal intensity) in approximately 1 hour.

4. Conclusions

In order to better comprehend the relationships between precipitation and landslide occurrence, rainfall data was analyzed along different range of intervals in terms of intensity, volume, and localization, using the landslide events around Kure City area in Hiroshima Prefecture) during the July 2018 heavy rain disasters as an investigation event.

Analysis of rainfall data in 2016 through 2019 demonstrated that the mean annual precipitation (MAP) amounts to about 2,152 mm in the sampled area. Considering spatial distribution of rainfall volumes around the study area, the XRAIN data shows that precipitation volumes are highly localized with intense rainfall values being concentrated in locations of elevated topography. Areas associated with these intense rainfall values seem to be closely related to high landslide density, except for areas with peak rainfall volumes associated to high altitude areas usually referent to bedrock-weathered mountain peaks and extremely steep slopes, not prone to landslide activity.

Considering the rainfall events of the July 2018 disasters, it was observed that Kure area experienced heavy continuous rainfall starting at 8:30 AM of July 5th, a condition which continued for about 47 hours until cease of rainfall at 7:30 AM of July 7th. XRAIN data shows that the precipitation accumulated up to

368 mm, and that the mean rainfall intensity was of 7.8 mm/h. There were two particular peaks of rainfall intensity, one 35 hours into the event at 7:30 PM of July 6th, when rainfall intensity reached 47 mm/h, and another 44 hours into the event, at 4:30 AM of July 7th, when rainfall intensity reached 40 mm/h. These peaks are associated to high landslide activity according to records of the disasters.

In this research, the relationship of both short and long-range rainfall data and landslide triggering was evidenced in spatial and chronological analysis, where landslide activity was found associated to areas with typically high precipitation values, as well as to periods in time correlated to peak intensity rainfall events after a particularly long duration of continuous precipitation. Recommendations for future studies in the subject include investigating the apparent quantitative disparities between XRAIN rainfall data and common rain gauge measurement station data, which was evidenced in this study. Also, performing similar analysis for areas with wider (chronologically and spatially) data ranges.

Declarations

Availability of data and materials

The datasets generated and/or analyzed during the current study cannot be made available with this manuscript because we have also used publicly available XRAIN data (from https://diasjp.net/en/ only after registration) but are available from the corresponding author upon request.

Competing interests

The authors declare that they have no competing interests.

Funding

There was no funding available for this research work.

Authors' contributions

DSRNJM (the first author) did the data analysis and made the basic concept for this paper while NPB (the second author) supervised the whole research work, crosschecked the results and discussion text, and guided DSRNJM several times in finalizing the article.

Acknowledgements

The immensely valuable free access to XRAIN data, widely utilized as a main item in this research was kindly permitted to by the Data Integration and Analysis System (DIAS) office, of The University of Tokyo. This research would not have been possible without the scholarship provided to the first author by the Ministry of Education, Culture, Sports, Science and Technology (MEXT) of Japan.

References

1. Canavesi, V.; Camarinha, P. I. M.; Algarve, V. R.; Carneiro, R. L. C.; Alvalá, R. C. S. 2013. Análise da susceptibilidade a deslizamentos de terra: estudo de caso de Paraibuna, SP. In: SIMPÓSIO BRASILEIRO DE SENSORIAMENTO REMOTO, 16. (SBSR), 2013, Foz do Iguaçu.
2. Caine, N. (1980) The Rainfall Intensity - Duration Control of Shallow Landslides and Debris Flows, Geografiska Annaler: Series A, Physical Geography, 62:1–2, 23–27.
3. Centre for Research on the Epidemiology of Disasters (2017). Economic losses, poverty & disasters 1998–2017. United Nations Office for Disaster Risk Reduction. Available at: < https://www.preventionweb.net/files/61119_credeconomiclosses.pdf>.
4. Chigira, M. (2001). Micro-sheeting of granite and its relationship with landsliding specifically after the heavy rainstorm in June 1999, Hiroshima Prefecture, Japan. Engineering Geology, 59, 219–231.
5. Dahal, R. K.; Hasegawa, S. (2008). Representative rainfall thresholds for landslides in the Nepal Himalaya, Geomorphology, 100 (3–4), 429–443.
6. Dahal, R. K. (2012). Rainfall-induced Landslides in Nepal. International Journal of Erosion Control Engineering, 5(1), 1–8.
7. Dai, F.; Lee, C.; & Ngai, Y.; (2002). Landslide risk assessment and management: an overview. Engineering Geology, 64(1), 65–87.
8. Geertsema, M.; Highland, L.; Vaugeouis, L. (2009). Environmental Impact of Landslides. In: Sassa, K.; Canuti, P.; (eds) Landslides – Disaster Risk Reduction. Springer, Berlin, Heidelberg.
9. Geospatial Information Authority of Japan (2018). “Information on heavy rain in July 2018” (translated title). Ministry of Land, Infrastructure, Transport and Tourism. Available at < https://www.gsi.go.jp/BOUSAI/H30.taihuu7gou.html>. Accessed in June 2020.
10. Guidicini, G.; Iwasa, O.Y. (1977) Tentative correlation between rainfall and landslides in a humid tropical environment. Bulletin of the International Association of Engineering Geology 16, 13–20.
11. Guzzetti, F.; Cardinali, M.; Reichenbach, P. (1996). The Influence of Structural Setting and Lithology on Landslide Type and Pattern. Environmental & Engineering Geoscience, II (4), 531–555.
12. Guzzetti, F.; Peruccacci, S.; Rossi, M.; Stark, C. P. (2007). Rainfall thresholds for the initiation of landslides in central and southern Europe. Meteorology and Atmospheric Physics, 98(3–4), 239–267.
13. Highland, L.M.; and Bobrowsky, P. (2008). The landslide handbook—A guide to understanding landslides: Reston, Virginia, U.S. Geological Survey Circular 1325, 129 p.
14. Hiroshima Prefectural Government (2018). “July 2018 heavy rain disasters” (translated title). Available at < https://www.sabo.pref.hiroshima.lg.jp/portal/sonota/sabo/pdf/234_H30_7gouusaigai.pdf>. Accessed in December 2021.
15. Japanese Meteorological Agency (2020). “Kure: average yearly and monthly values” (translated title). Available at < http://www.data.jma.go.jp/. Accessed in June 2020.

16. Kamada, M.; Nakagoshi, N. (1996). Landscape structure and the disturbance regime at three rural regions in Hiroshima Prefecture, Japan. Landscape Ecol 11, 15–25.
17. Matsushi Y.; Matsuzaki H.; Makino H. (2014). Testing models of landform evolution by determining the denudation rates of mountainous watersheds using terrestrial cosmogenic nuclides. Trans. Jpn. Geomorphol. Union,35, 165–185.
18. Ministry of Land, Infrastructure, Transport and Tourism (2018). “Information related to sediment-related disasters caused by heavy rains in July 2018” (translated title). Available at < https://www.mlit.go.jp/river/sabo/H30_07gouu.html>. Access in June 2020.
19. Osanai, N.; Tomita, Y.; Akiyama, K.; Matsushita, T. (2009). Technical note of National Institute for Land and Infrastructure Management No.530. National Institute for Land and Infrastructure Management, Ministry of Land, Infrastructure, Transport and Tourism, Japan.
20. Petley, D. (2012). Global patterns of loss of life from landslides. Geology, 40(10), 927–930.
21. Ushiyama M.; Ohido S.; Takara K. (2001). The critical line for sediment disaster warning based on precipitation data in Hiroshima Prefecture in June 1999. “Collection of River Technology Papers, Volume 7” (translated title).
22. Wang, F.; Wu, Y. -H.; Yang, H.; Tanida, Y.; Kamei, A. (2015). Preliminary investigation of the 20 August 2014 debris flows triggered by a severe rainstorm in Hiroshima City, Japan. Geoenvironmental Disasters, 2(1).
23. Yahoo Maps (2020). “Map of Kure City, Hiroshima Prefecture” (translated title). Yahoo Japan Corporation. Available at < https://map.yahoo.co.jp/>. Accessed in June 2020.
24. Yamada, N.; Higashimoto, S.; Mizuno, K.; Hiroshima, T.; Suda, Y. (1986). Hiroshima 1:200,000 geological map, NI-53-33. Geological Survey of Japan.
25. Yilmaz, I. (2009). Landslide susceptibility mapping using frequency ratio, logistic regression, artificial neural networks and their comparison: A case study from Kat landslides (Tokat—Turkey). Computers & Geosciences, 35(6), 1125–1138.

Figures

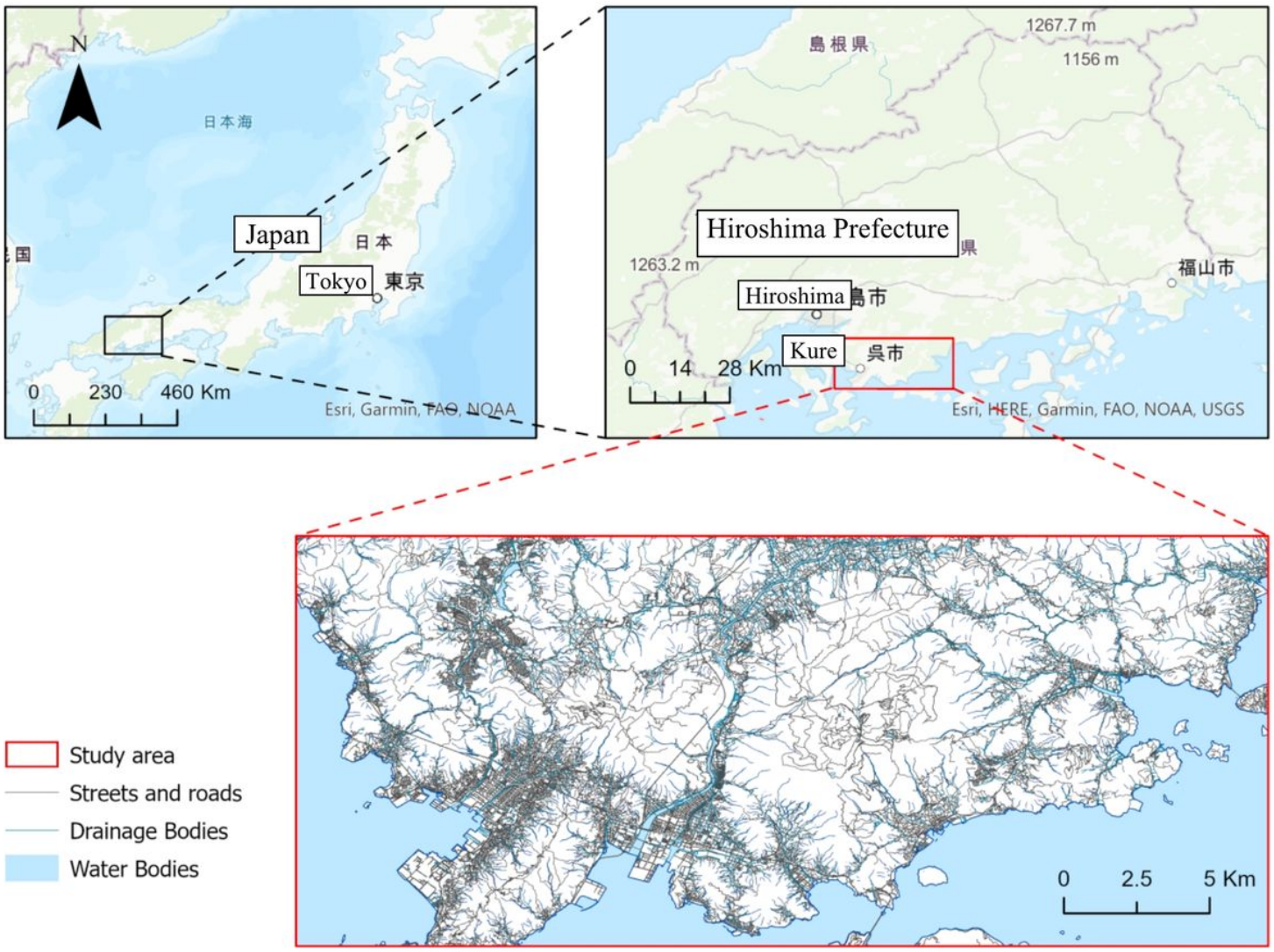

Figure 1

Study area around Kure, Hiroshima Prefecture, Southwest Japan. Source: Yahoo Maps (2020); Hiroshima Prefecture (2018).

Figure 2

Aerial pictures of the aftermath from multiple landslides occurred in the July 2018 heavy rain-induced disasters in Kure City, Hiroshima Prefecture. Source: Hiroshima Prefectural Government (2018).

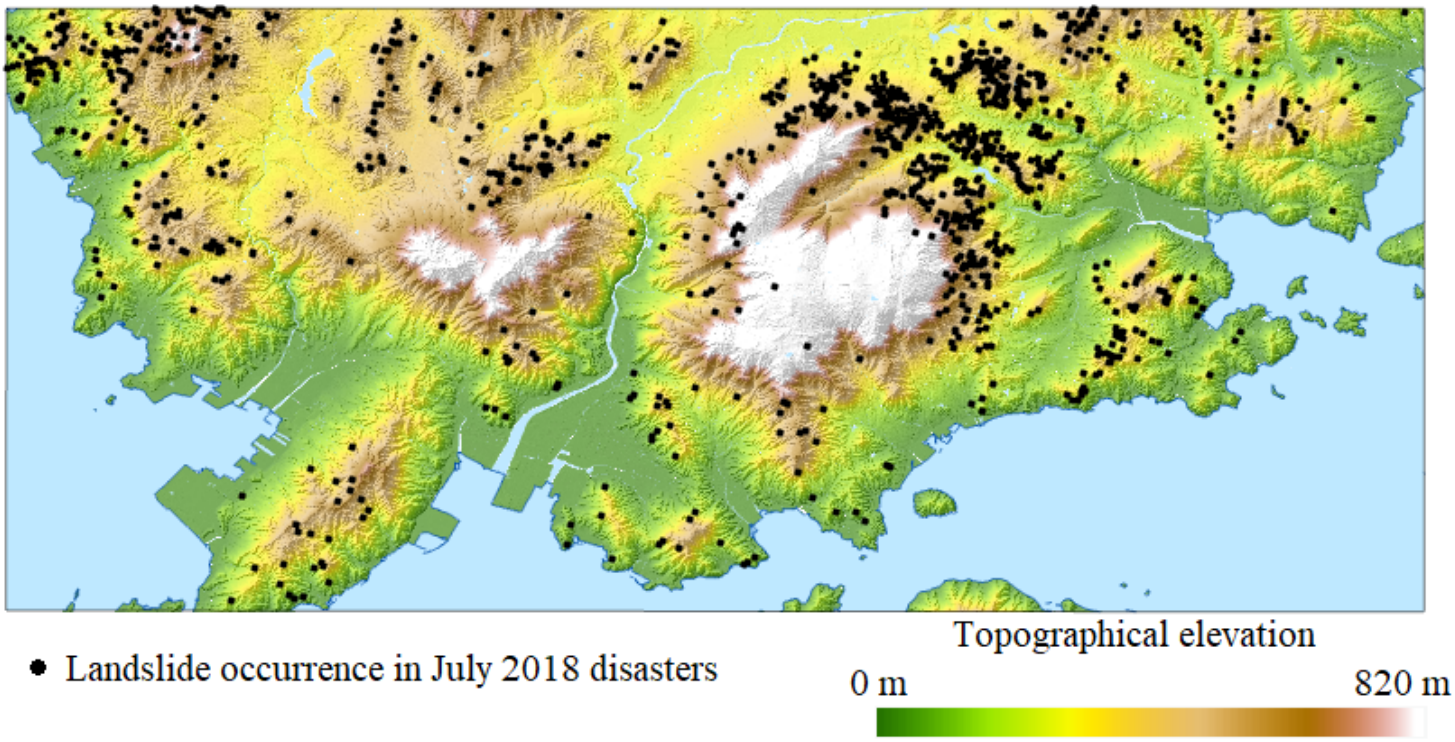

Figure 3

DEM of the study area along with landslide occurrence in the July 2018 disasters.

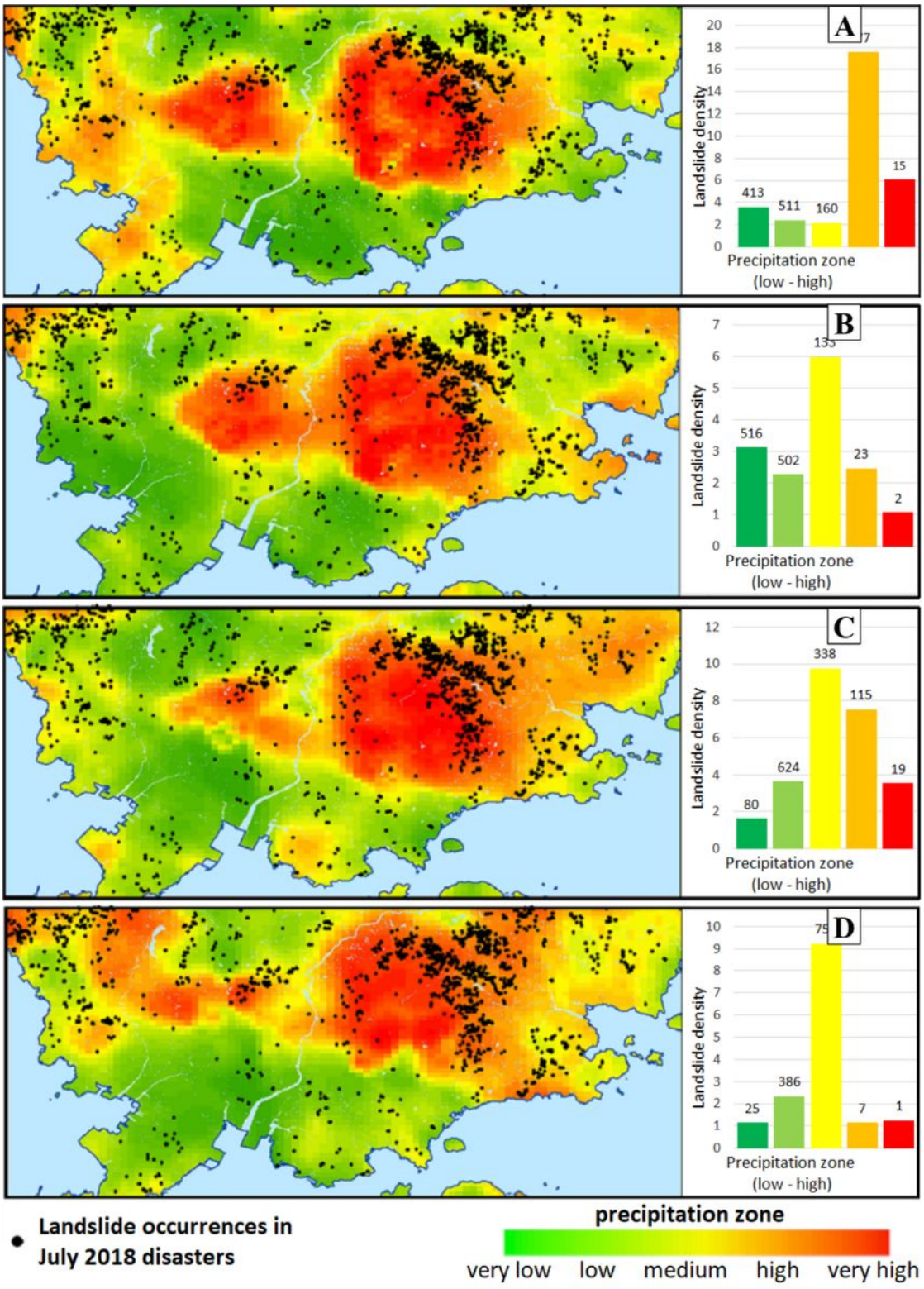

Figure 4

Localized annual precipitation for the years of (A) 2016; (B) 2017; (C) 2018; and (D) 2019 (XRAIN radar-acquired data) along with landslide occurrence points recorded from the July 2018 disasters in the study area of Kure City as black dots, as well as bar graphs indicating landslide density per precipitation zone (from green to red: very low; low; medium; high; very high) for each of the referenced years. Values above each bar represent the number of landslides in the respective zone.

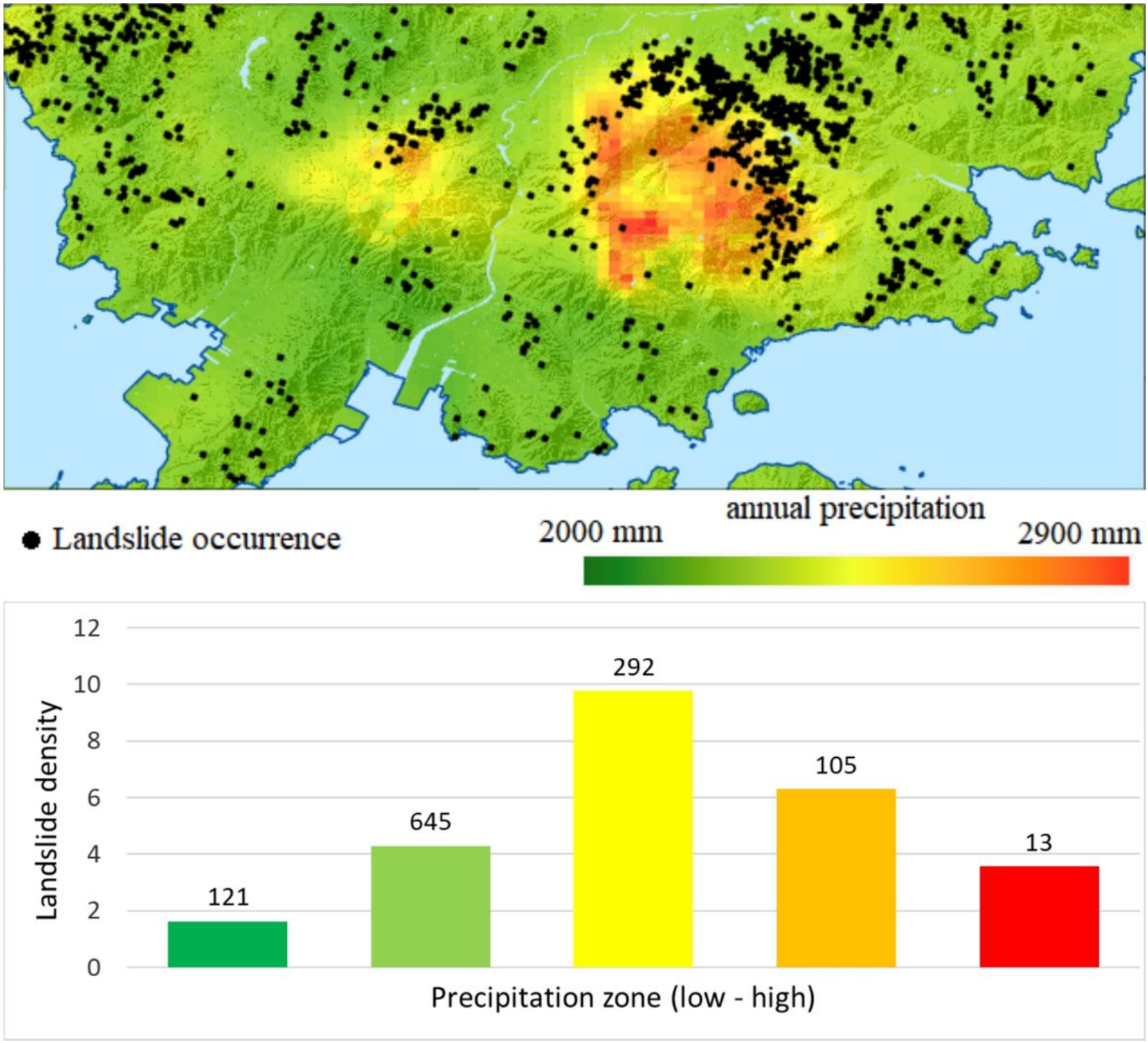

Figure 5

Localized mean annual precipitation for the years of 2016 and 2019 (XRAIN radar-acquired data) along with landslide occurrence points recorded from the July 2018 disasters in the study area of Kure City, as well as bar graphs indicating landslide density in each precipitation zone (from green to red: very low; low; medium; high; very high). Values above each bar represent the number of landslides in the respective zone. It is observed that localization patterns change very little over the years, and rainfall is particularly concentrated in topographically elevated areas.

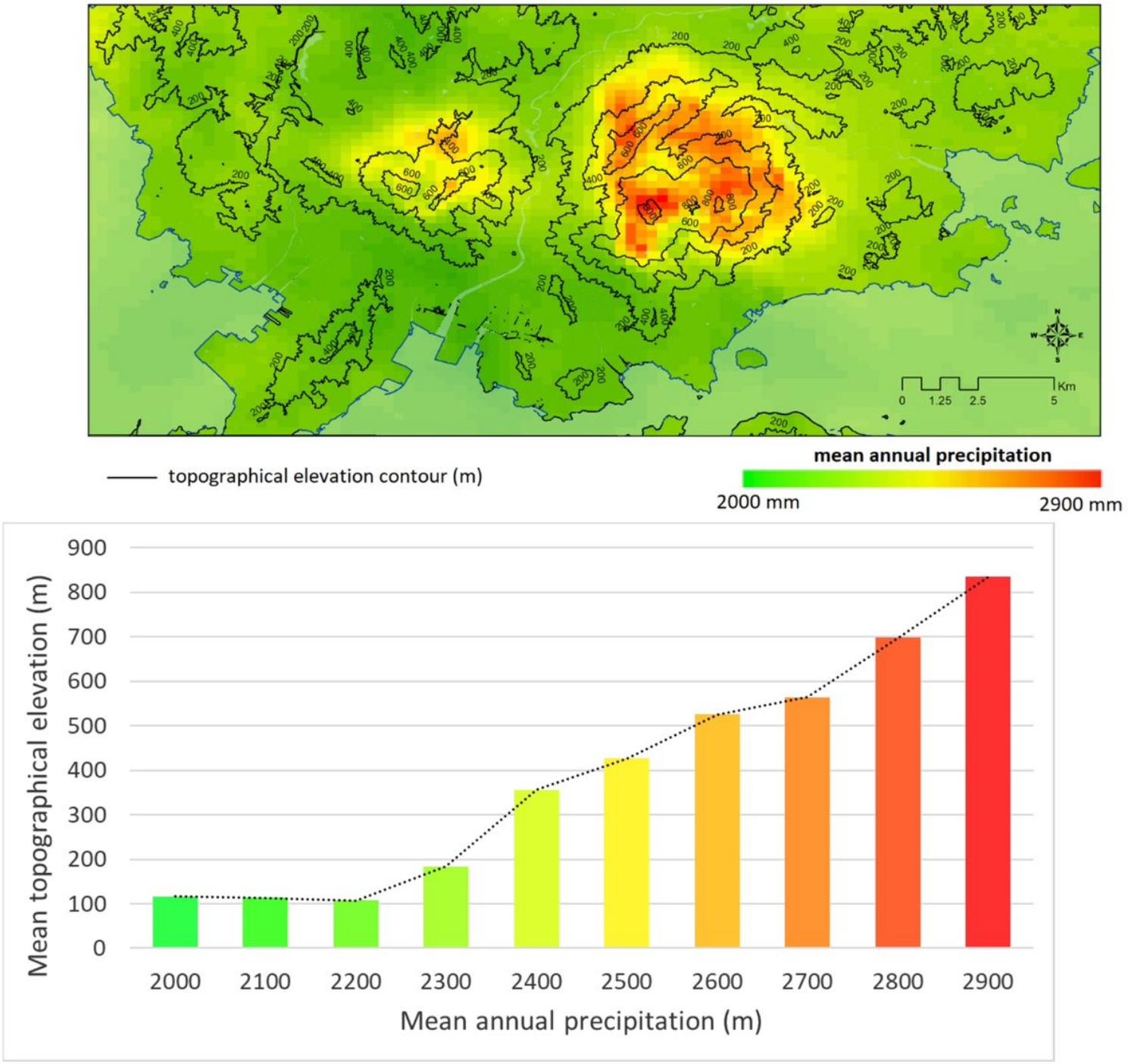

Figure 6

Relationship between MAP from 2016 to 2019 (represented by green-red color grading) and topographical elevation (represented by contour lines), as well as bar graphs indicating the mean topographical in relation to the mean annual precipitation. It is noticeable that high precipitation values are concentrated in peak elevation locations.

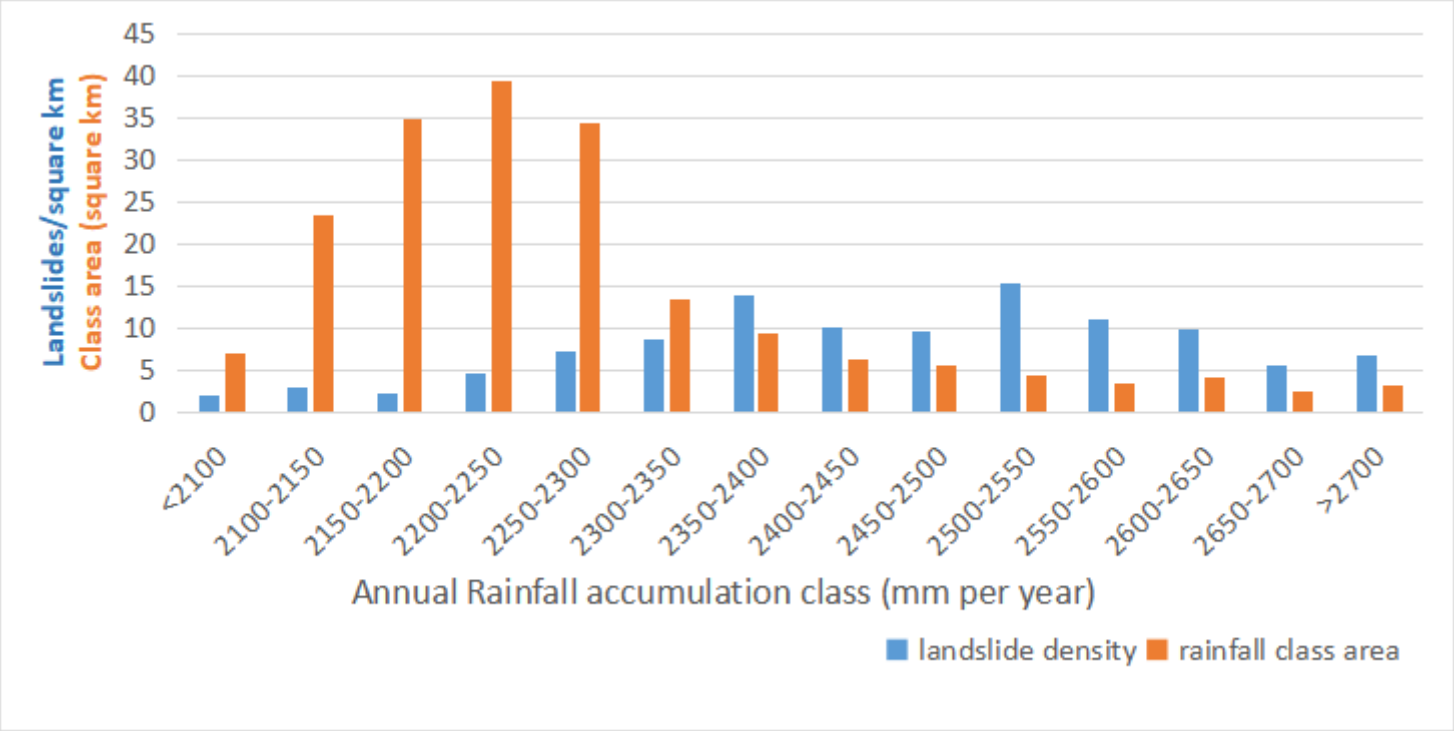

Figure 7

Relationship between landslide density per Mean annual precipitation class (XRAIN data), along with class area. It is observed that landslide density peaks around intermediate to high values.

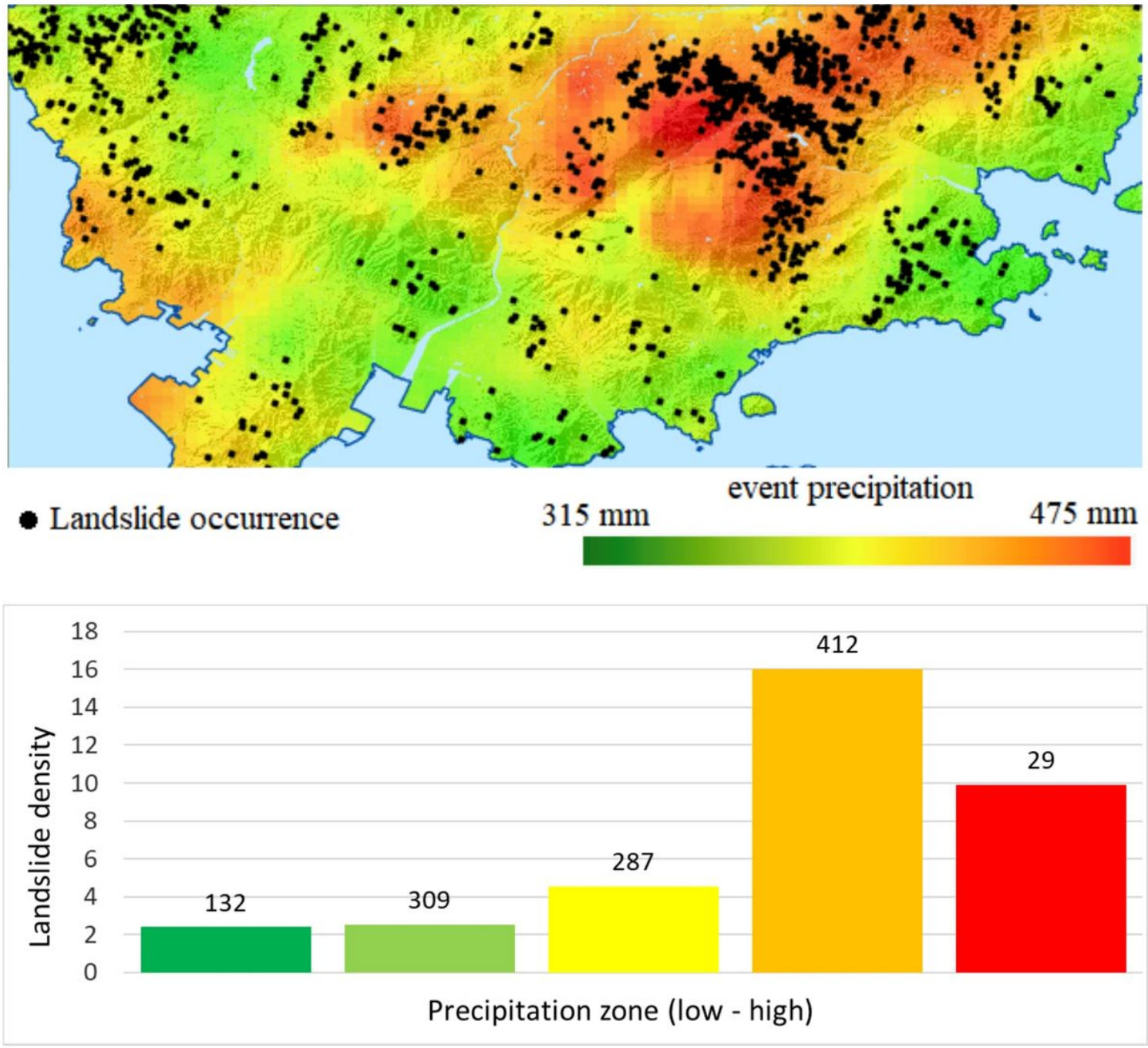

Figure 8

Localized accumulated rainfall between July 5th 8:30 AM to July 7th 7:30 AM in the study area and accompanying bar graphs of landslide density per precipitation zone (from green to red: very low; low; medium; high; very high). Values above each bar represent the number of landslides in the respective zone. Although the localization follows the same pattern as annual rainfall, there is a slightly closer relationship with landslide activity.

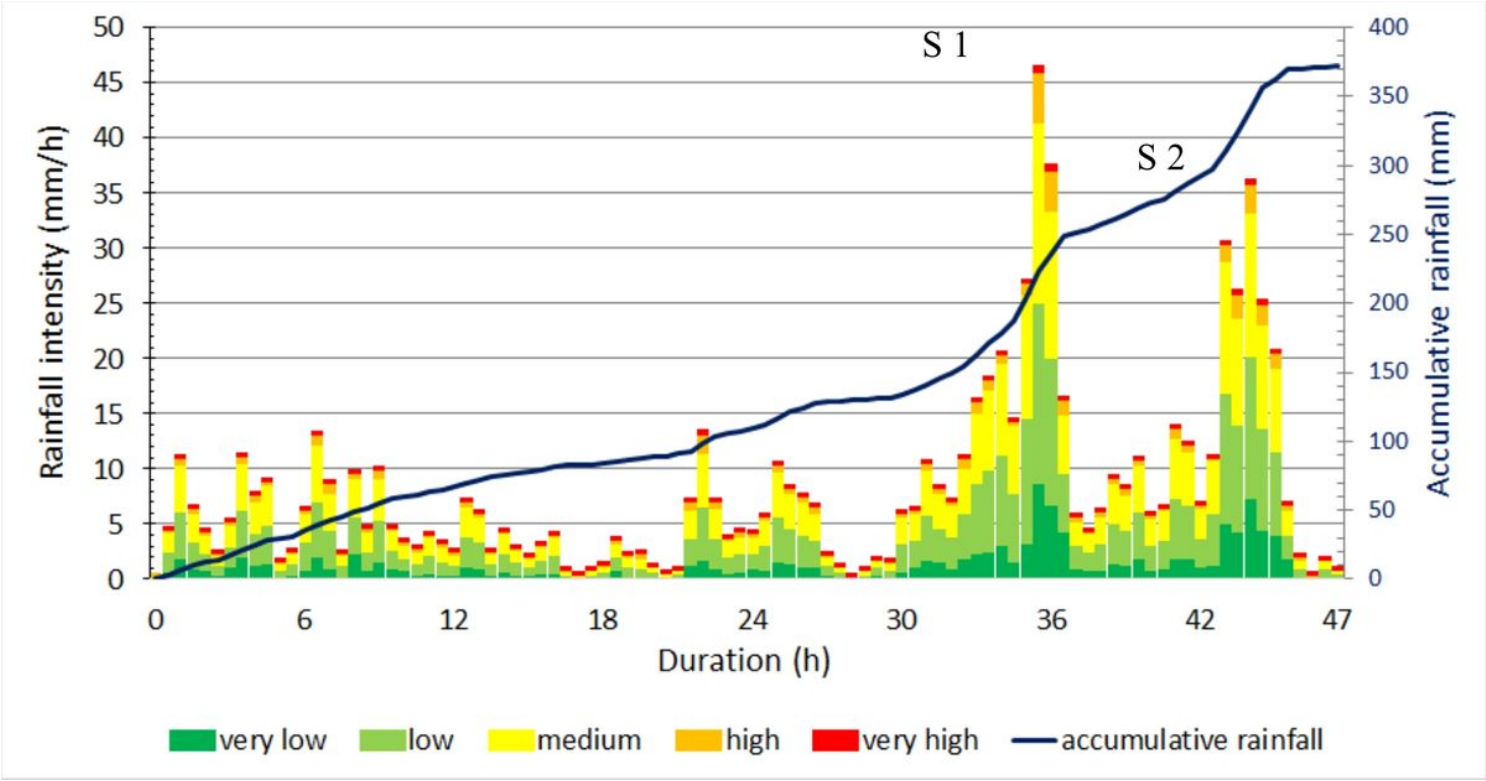

Figure 9

Graph illustrating the history of rainfall over the course of 47 hours from July 5th 8:30 AM to July 7th 7:30 AM in the study area, with respective share of precipitation class zones to the total rainfall in the area (from very low to low). S1 and S2 indicate, respectively, subevent 1 (7:30 PM of July 6th) and subevent 2 (4:30 AM of July 7th) of the July 2018 disasters.

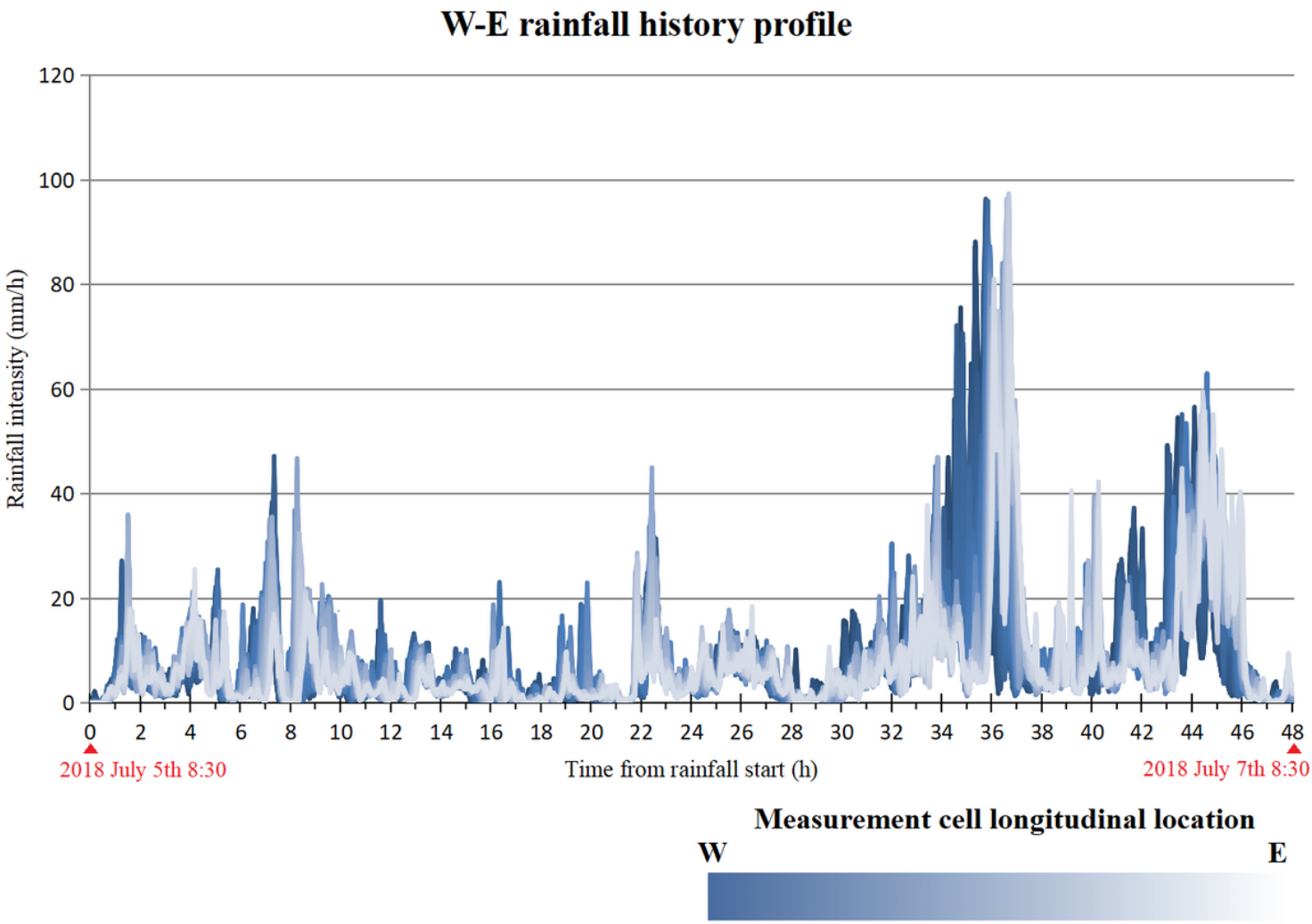

Figure 10

Collection of 92 graphs of rainfall intensity history during the July 2018 disaster event, along a longitudinal profile located on latitudinal center of the study area. An interval of about 1 hour is noticeable between intensity peaks of the westward and eastward extremities of the study area.